

Multilayer ANN indoor location system with area division in WLAN environment

Mu Zhou*, Yubin Xu, and Li Tang

School of Electronics and Information Engineering, Harbin Institute of Technology, Harbin 150001, P. R. China

Abstract: An indoor location system based on multilayer artificial neural network (ANN) with area division is proposed. The characteristics of recorded signal strength (RSS), or signal to noise ratio (SNR) from each available access points (APs), are utilized to establish the radio map in the off-line phase. And in the on-line phase, the two or three dimensional coordinates of mobile terminals (MTs) are estimated according to the similarity between the new recorded RSS or SNR and fingerprints pre-stored in radio map. Although the feed-forward ANN with three layers is sufficient to describe any nonlinear mapping relationship between inputs and outputs with finite discontinuous points, the efficient inputs for better training performances are difficult to be determined because of complex and dynamic indoor environment. Then, the discussion of distance relativity for different signal characteristics and optimal strategies for multi-mode phenomenon avoidance is presented. And also, the feasibility and effectiveness of this method are verified based on the experimental comparison with normal ANN without area division, K-nearest neighbor (KNN) and probability methods in typical office environment.

Keywords: indoor location, artificial neural network, multilayer structure, multi-mode, relativity.

DOI: 10.3969/j.issn.1004-4132.2010.05.028

1. Introduction

With the increasing interests of ubiquitous context-aware requirements, indoor location services have been paid much more attention recently [1]. Not only for the military uses, but also civil applications, the location awareness applications include, but not limited to, emergency rescue, finding and tracking, guiding and escorting system, positioning of entities in modern buildings [2–5].

Currently, the localization algorithm can be classified into distance method and pattern recognition method. For the distance method, there are global positioning system (GPS), cellular systems for outdoor environment [6,7] and proximity detection (PD), time of arrival (TOA), time

difference of arrival (TDOA) and angle of arrival (AOA) methods. Because of the non line of sight (NLOS) and multi-path effects which are induced by the building geometry, human body absorption, adjacent frequency interference, dynamic environments and requirement of special infrastructures, the scope of their application is restricted [8,9]. However, along with the increase of AP in actual indoor environment and emergence of non-registered 2.4 GHz ISM band with free wireless license for 802.11 b/g protocol [10], a WLAN indoor location technology based on pattern recognition has been extensively researched and widely used for the current laptop or personal digital assistant (PDA).

The WLAN location system by pattern recognition algorithm can be separated into two independent phases, the off-line phase (calibration phase) and on-line phase (estimation phase) [11]. In the off-line phase, the samples of beacon signal strength at separate referent points (RPs) are recorded to establish radio map. And in the on-line phase, the MT's coordinates are estimated [12].

According to the reasons of nonlinear mapping ability, parallel distributed processing, adaptive self-learning, data fusion and multivariable structure, ANN becomes one of efficient tools for coordinates' estimation [13], with merits of reducing the time cost for location system layout, saving the storage cost for radio map establishment and enhancing the real-time positioning capacity in on-line phase [14–16].

However, the selection of ANN training samples and the multi-mode phenomenon significantly affect the performance of ANN indoor location systems. So in order to bridge this gap, five SNR characteristic values are analyzed for selecting the optimal distance dependent inputs for ANN training and constructing a multilayer ANN indoor location system. Furthermore, the avoidance strategy for multi-mode phenomenon is also presented to guarantee the unique of fingerprints pre-stored in radio map.

The remainder of this paper is organized as follows. In Section 2, the fundamental structure of three-layer feed-

Manuscript received May 19, 2009.

*Corresponding author.

This work was supported by the National High Technology Research and Development Program of China (863 Program)(2008AA12Z305).

forward ANN is described. Section 3 presents a multilayer ANN structure based on discussion of distance dependence for different SNR characteristics. Section 4 analyzes the common multi-mode phenomenon. In Section 5, the performance of multilayer ANN is compared with ANN without area division, KNN and probability methods. Section 6 concludes this paper.

2. Fundamental model

2.1 Proposal of ANN structure

The traditional methods, such as nearest neighbor (NN), KNN and probabilistic methods based on fingerprinting architecture, improve the location accuracy and precision in some special conditions and also face the challenges of the time and storage costs for the WLAN signal acquisition and processing, the adaptability for different complex indoor environments. Although the theoretical propagation model revealing the relationship between RSS or SNR with RPs saves on the establishment time for the radio map, the location performance becomes terrible because of the complex and dynamic indoor environment that is different from free space.

So, in order to balance the location performance and system establishment cost, the ANN structure is utilized to construct an intelligent and efficient indoor location system. Furthermore, the accuracy performance of this method will not depend on the number of detectable APs, but distance relativity between training inputs of output coordinates.

2.2 Three-layer feed-forward ANN

MT's coordinates' estimation, following three factors should be focused on firstly.

(a) Topological structure of ANN

Three-layer feed-forward ANN is selected in this paper, which has been demonstrated to be sufficient to approximate any continuous function within the desired accuracy [17]. But the number of hidden perceptrons can only determined by experiments without any theoretical guidance or existing analytic expression supported [18].

(b) Initial value of weights and biases

In order to reduce training time, avoid low efficiency and achieve global optimum, these values should be properly set to make the input value for each perceptron close to value 0, and the state transition function $f(x) = \frac{1}{1 + e^{-x}}$

has the steepest variation.

(c) Modification of weights and biases

Back propagation (BP) with conjugate gradient method is utilized to minimize the target training error because of the differentiability of this model and efficiency purpose.

And also, the transfer process of three-layer feed-forward ANN with N inputs, T hidden perceptrons and 2 outputs is shown by

$$\left\{ \begin{array}{l} x_{j,p}^l = \sum_{j=1}^{N_{l-1}} \omega_{ij}^{l-1,l} y_{j,p}^{l-1} - \theta_j^{l-1,l}, \text{ for } l = 1, 2 \\ y_{j,p}^l = f(x_{j,p}^l) = \frac{1}{1 + e^{-x_{j,p}^l}}, \\ \text{for } 0 < f(x_{j,p}^l) < 1 \\ N_l = \begin{cases} N, & l = 0 \\ T, & l = 1 \end{cases} \\ j = \begin{cases} 1, \dots, T, & l = 1 \\ 1 \text{ or } 2, & l = 2 \end{cases} \end{array} \right. \quad (1)$$

where $\theta_j^{l-1,l}$ ($l = 1, 2$) denotes the biases determining the active or negative state of perceptron in layer l . $\omega_{ij}^{l-1,l}$ denotes the connection weight from layer $l-1$ to l . $x_{j,p}^l$ ($l = 1, 2$) denotes the output value of perceptron j in layer l for sample p . $y_{j,p}^l$ ($l = 0, 1$) denotes the input value from perceptron j in layer l for sample p .

2.3 ANN training

In the ANN training process, based on the modification of weights and biases, the training error E_{train} defined in (2) should be minimized.

$$E_{\text{train}} = \frac{1}{2} \sum_p \|Y_p^2 - Z_p\|^2 = \frac{1}{2} \sum_{p=1}^P \sum_{j=1}^2 (y_{j,p}^2 - z_{j,p})^2 \quad (2)$$

where P denotes the number of training samples. $z_{1,p}$ and $z_{2,p}$ denote the expected x and y coordinates respectively in training phase. $y_{1,p}^2$ and $y_{2,p}^2$ denote the output x and y coordinates respectively.

The iterative process for the optimal weights and biases is calculated by

$$\left\{ \begin{array}{l} \omega_{ij}^{l-1,l}(k+1) = \omega_{ij}^{l-1,l}(k) - \frac{\alpha \partial E_{\text{train}}}{\partial \omega_{ij}^{l-1,l}(k)} = \\ \omega_{ij}^{l-1,l}(k) - \alpha \sum_{p=1}^P \delta_{j,p}^l(k) y_{j,p}^{l-1}(k) \\ \theta_j^{l-1,l}(k+1) = \theta_j^{l-1,l}(k) - \beta \sum_{p=1}^P \delta_{j,p}^l(k) y_{j,p}^{l-1}(k) \\ \delta_{j,p}^l(k) = \begin{cases} f'[x_{j,p}^l(k)] \sum_{m=1}^2 \delta_{m,p}^{l+1}(k) \omega_{jm}^{l,l+1}(k), & l = 1 \\ [y_{j,p}^l(k) - z_{j,p}] f'[x_{j,p}^l(k)], & l = 2 \end{cases} \\ i = \begin{cases} 1, \dots, N, & l = 1 \\ 1, \dots, T, & l = 2 \end{cases} \\ j = \begin{cases} 1, \dots, T, & l = 1 \\ 1 \text{ or } 2, & l = 2 \end{cases} \text{ for } k \leq K_{\text{iter}} \end{array} \right. \quad (3)$$

where α and β denote the learning rate of $\omega_{ij}^{l-1,l}$ and $\theta_j^{l-1,l}$ respectively. K_{iter} denotes the maximum iteration number.

2.4 Generalization enhancement

Generalization should be significantly considered for any ANN based intelligent systems. Because the training error can be limited to a very small value with a large number of iterations, but when new samples are presented to the trained ANN, the error may be enlarged with terrible generalization ability, which is also called over fitting [19–21]. So, in order to improve the generalization ability of multilayer ANN indoor location systems, early stopping and Bayesian regularization methods are utilized in this paper.

(a) Early stopping

Samples recorded at RPs are divided into training and validation subsets. Normally, the validation error decreases during the initial phase of training, but if the network is over fitted, the error on this set will significantly begin to increase. As long as the validation error rises for a specified number of iterations, the training process is stopped, and the weights and biases at the minimum of the validation error are returned. In this paper, the proportions of training and validation sets are set as 80% and 20% respectively.

(b) Bayesian regularization

Regularization method can significantly enhance ANN generalization based on the modification on target training error $E_{\text{mod,train}}$ by adding a term that consists of the mean of the sum of squares of network weights and biases that is shown in (4), the response is smoother and less likely to be over fitting.

$$\begin{cases} E_{\text{mod,train}} = \lambda E_{\text{train}} + (1 - \lambda)(\text{ms}\omega + \text{ms}\theta) \\ \text{ms}\omega = \frac{1}{N_\omega} \sum_{i=1}^{N_\omega} \omega_i^2 \\ \text{ms}\theta = \frac{1}{N_\theta} \sum_{j=1}^{N_\theta} \theta_j^2 \end{cases} \quad (4)$$

where the performance ratio $\lambda = 0.5$ gives equal weights E_{train} and mean square weights and biases. N_ω and N_θ denote the number of weights and biases.

3. Area division

3.1 Purpose

The ANN based indoor location system with area division can provide the following three advantages.

(a) Feasibility is guaranteed by the multiple ANN subsystems with parallel processing.

In this paper, the clustering ability of ANN is utilized for the purpose of coordinates' estimation. However, clustering rules by low dimensional signal vectors are difficult to be determined especially for the target location area with large dimensions and irregular shape. And also, because of the continuous mapping relationship between input signals and output coordinates, the probability of estimated position in impossible areas will be significantly improved for single ANN system. So in order to bridge this gap, multiple ANN with area division is presented to decrease clustering rules, reduce impossible probability and guarantee feasibility.

(b) Optimization of ANN training samples is beneficial for the accuracy improvement.

For the real indoor environment, the recorded signals are mixed with signals from different APs and noise, because of the only three non-overlapping channels by 802.11 b/g and adjacent frequency interference in band 2.4GHz. Then, the ANN system with area division by eliminating the strong signals and noise with poor distance relativity can significantly improve training performance.

(c) Reduce the dimensions of ANN inputs to increase positioning efficiency.

There are five signal characteristics, the mean, median, maximum, minimum and variance values for each AP. If all the characteristics are selected as the ANN inputs ($5 \times N_{\text{AP}}$), the number of perceptrons in hidden layer is difficult to be determined, and also, the over fitting phenomenon is much more likely to happen. Therefore, in order to improve the location efficiency and accuracy, the characteristics which are much more depended on the distance variation will be selected as the ANN inputs.

3.2 Distance relativity

For the purpose of selecting the best distance dependent characteristics as the input vectors of ANN for different divided target areas, the distribution characteristics of SNR should be analyzed firstly. Then, based on the relativity calculation of the X and Y direction in a flat, the target location area is divided into separate regions with optimal ANN based location subsystems for the purpose of improving indoor location performance.

The dimensions of environment are 66.43×24.9 m². Walls are made of bricks with large windows in aluminum frames, and doors are made of metal. There are 9 D-link DWL-2100AP APs which are denoted by AP1, AP2, ..., AP9 fixed at the height of 2 m in the same floor. These APs supports IEEE 802.11g standard with data rates up to 54 Mbps, and the SNR samples are recorded by a laptop 1.2 m high. The table tennis room is selected as test environment shown in Fig. 1 and Fig. 2 for its regular shape

and excellent coverage performance by AP1, 2, 3, 8 and 9. And also, Y coordinates in X direction are denoted by A, B, ..., H. X coordinates in Y direction are denoted by 1, 2, ..., 9.

The five characteristics of SNR from AP3 at test points are shown in Fig. 3. And the distribution characteristics of SNR from other four APs which can be detected in the target location area can be acquired in the same way.

According to Fig. 3, the distribution characteristics of mean, median, maximum and minimum values of SNR from AP3 are quite similar, and the variance value changes greatly without any regularity, which is not beneficial to be utilized for location algorithm. In addition, because of the lack of enough signal samples for statistical calculation in the real-time positioning condition, median, maximum and minimum performs terrible compared with the mean value. And also, the mean values of SNR from other 4 APs which can be detected in the target location area are separately shown by Fig. 4.



Fig. 1 Photographs of APs and receiver

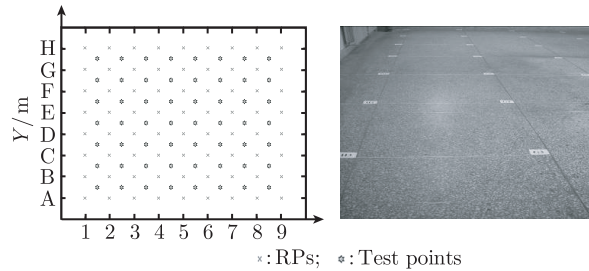


Fig. 2 Flat of experimental environment

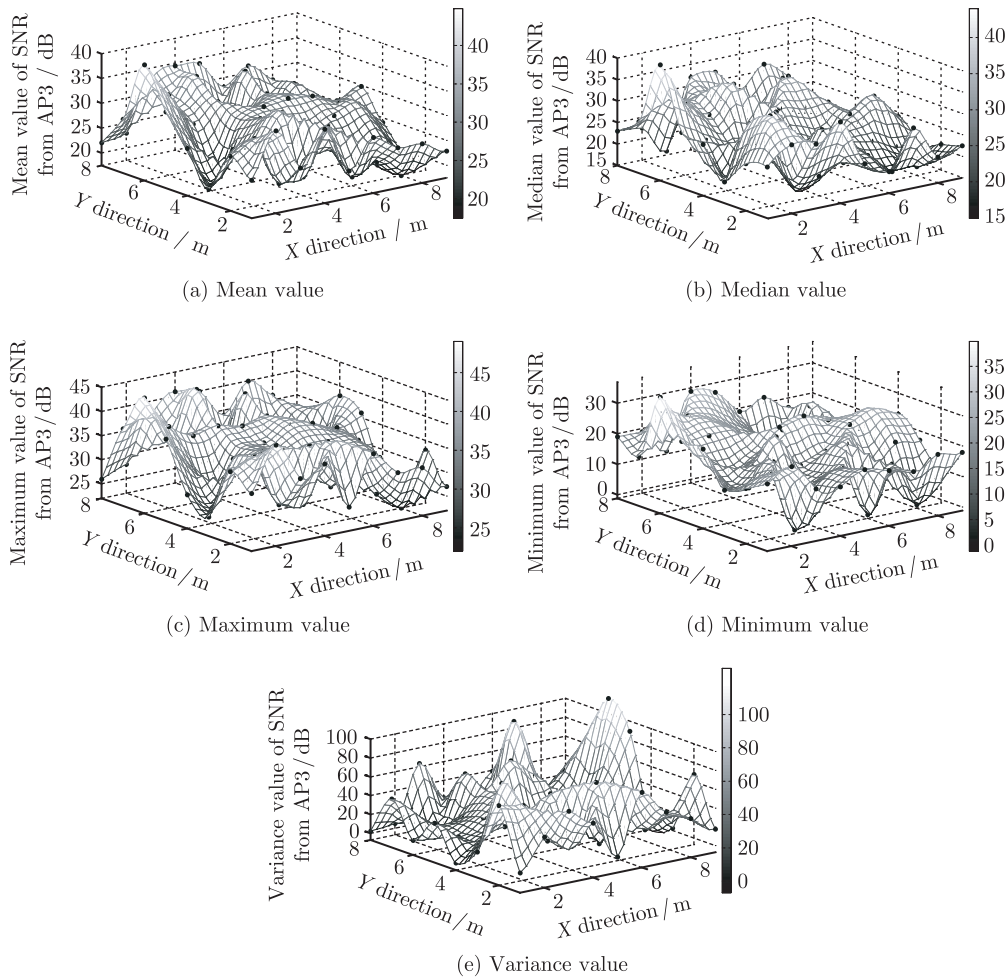


Fig. 3 Five characteristics of SNR from AP3

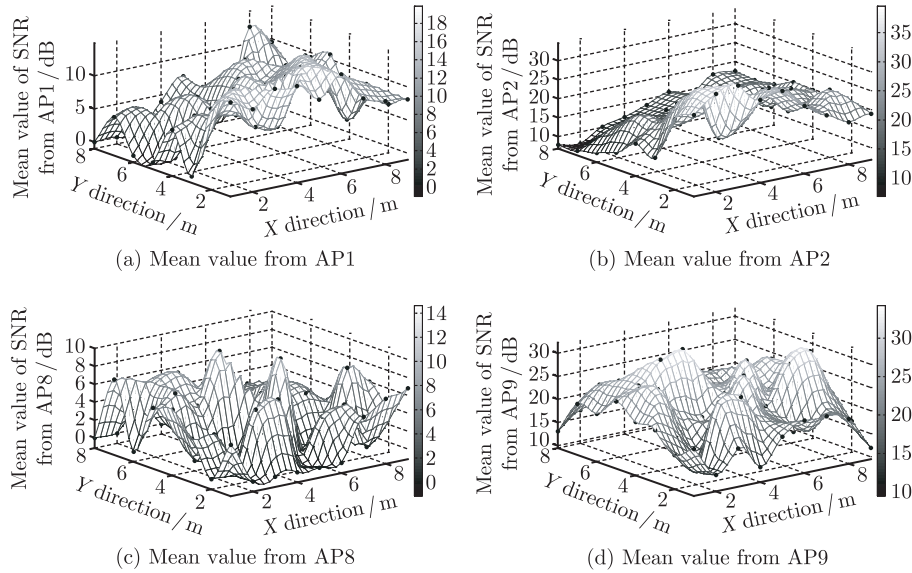


Fig. 4 Mean value of SNR from AP*i* (*i* = 1, 2, 8, 9)

Therefore, distance relativities between mean value and X or Y coordinates $R_{k,X,j}$ and $R_{k,i,Y}$ are calculated by

$$\left\{ \begin{aligned} R_{k,X,j} &= \frac{\left| \sum_{i=1}^9 (M_{k,i,j} - \overline{M_{k,j}})(i - \bar{i}) \right|}{\sqrt{\sum_{i=1}^9 (M_{k,i,j} - \overline{M_{k,j}})^2 \sum_{i=1}^9 (i - \bar{i})^2}}, \\ & j = 1, \dots, 8 \\ R_{k,i,Y} &= \frac{\left| \sum_{j=1}^8 (M_{k,i,j} - \overline{M_{k,i}})(j - \bar{j}) \right|}{\sqrt{\sum_{j=1}^8 (M_{k,i,j} - \overline{M_{k,i}})^2 \sum_{j=1}^8 (j - \bar{j})^2}}, \\ & i = 1, \dots, 9 \end{aligned} \right. \quad (5)$$

where $M_{k,i,j}$ denotes the mean value at RP (*i*, *j*) from

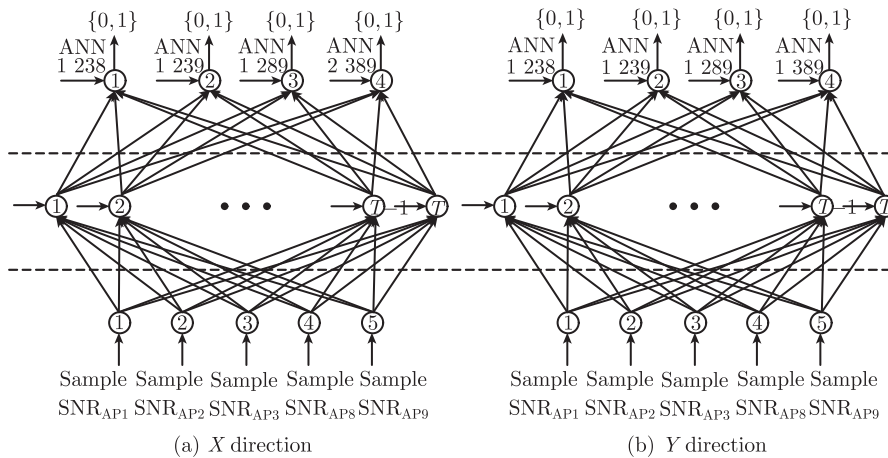


Fig. 5 Area division ANN in different directions

AP*k*. $\overline{M_{k,j}}$ and $\overline{M_{k,i}}$ denotes the mean value of $M_{k,i,j}$ with fixed Y and X coordinates respectively.

3.3 Area division strategy

The inputs with poorest distance relativity will be eliminated by the area division strategy. Therefore, 5 ANN subsystems presented by Table 1 will be constructed for different directions in the target location area.

After the area division by distance relativity, two three-layer feed-forward ANNs shown by Fig. 5 are constructed for the purpose of optimal ANN subsystems selection.

Table 1 Area division by distance relativity

ANN subsystems	Y coordinates in X direction	X coordinates in Y direction
ANN 1 238	A, B	1, 3, 6
ANN 1 239	D, F	5
ANN 1 289	E, H	2, 4, 8, 9
ANN 1 389	Null	7
ANN 2 389	C, G	Null

Coordinate $(4, F)$ is taken as an example, the target outputs are $(0, 1, 0, 0)$ and $(0, 0, 1, 0)$ respectively for area division ANNs in X and Y directions. In this situation, the membership degrees to ANN 1 239 (for X direction) and ANN 1 289 (for Y direction) are 1, but to the other ANN subsystems are 0.

3.4 Multilayer ANN location system

According to the foregoing discussion about the area division strategy, ANN subsystem determination and MT's coordinates' estimation process, the establishment of the

multilayer ANN indoor location system which is shown by Fig. 6 is necessary. Furthermore, five advantages for this multilayer system are listed below.

(a) The generalization ability of three-layer feed-forward ANN is guaranteed by the early stopping and Bayesian regularization methods presented by Section 2.4.

(b) Multiple subsystems are constructed for different divided areas with the distance relativity criterion to decrease the interference from strong signals with poor distance dependence discussed by Section 3.2.

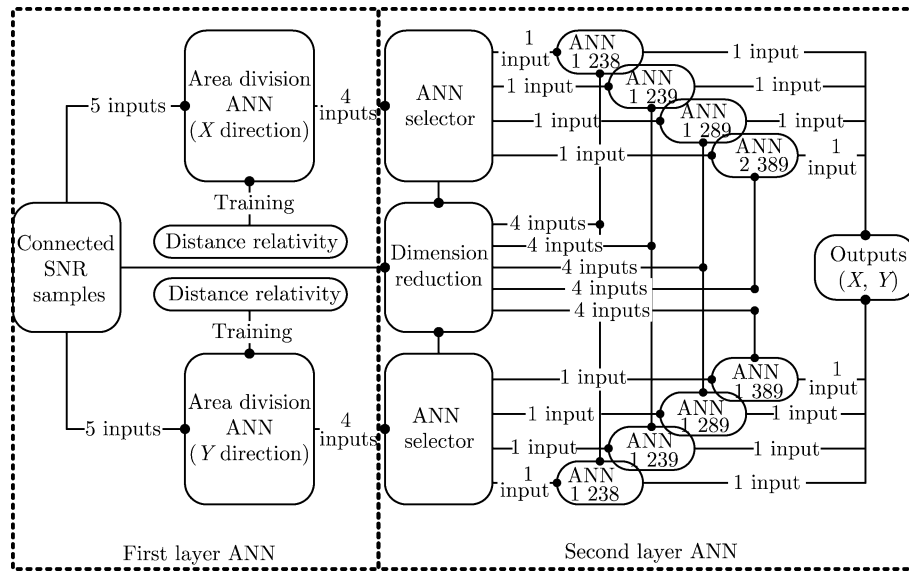


Fig. 6 Multilayer ANN indoor location system

(c) Training samples are optimized based on the avoidance of multi-mode phenomenon which will be further analyzed in Section 4.2.

(d) Multilayer ANN structure can reveal the definite physical meanings for connection relationship and improve system expansibility.

(e) Performance of the multilayer ANN structure can be verified in the real indoor environment with multi-path effect, human absorption and co-frequency interference.

Furthermore, the selection criterion of the ANN selector will be analyzed by Section 5.2 in detail. However, there are also two problems which should be considered for the multilayer ANN indoor location system.

(a) Reliability for the first layer ANN should be paid much more attention, because the selection of second layer ANN and final coordinates estimation is directly influenced by the performance of area division ANN.

(b) Linear correlation calculated by (5) is utilized to describe the dependence between signal strength and distance. However, in some real indoor environments, this lin-

ear relationship cannot be satisfied. In other words, some characteristics with poor linear correlation with distance may also perform well because of the nonlinear mapping ability.

4. Multi-mode phenomenon

4.1 Radio map

According to the reasons of special equipment which is needed by PD, TOA, TDOA and AOA methods, and the poor performance of the propagation model method, the fingerprint method based on the establishment of radio map is utilized in this paper. And the SNR samples recorded at separate RPs have been proved to be one of the best training vectors for ANN [22–24].

Furthermore, the following three reasons contribute the wide application of radio map.

(a) The continuing popularity of WLAN technology and applications, which means the utilization of basic facilities supporting 802.11 protocols will be paid much more attention.

(b) Because of the dynamic environment and multi-path

effect, the signal distribution cannot be accurately estimated by propagation model, and the relativity between attenuation of signal strength and distance apart from the AP to terminal is not obvious.

(c) Most of the current indoor location algorithms, no matter probabilistic or deterministic methods (such as NN or KNN methods), depend on the radio map which is established in the off-line phase. So, the fingerprint method is beneficial to the algorithm expansibility.

Obviously, the performance of the radio map based indoor location method depends on the characteristics of signal distribution. In other words, the noise comprised in signals and multi-mode phenomenon emerged in the process of signal recording significantly affect location accuracy. Noise with terrible distance dependence can be effectively eliminated by area division ANN which has been discussed by prior Section 3. So in this section, the characteristics of signal distributions will be analyzed for the purpose of avoiding this phenomenon as effectively as possible and improving location accuracy.

4.2 Characteristics of signal distribution

Because of the dynamic multi-path effect, interference with adjacent receivers, different types of wireless network cards, connection state of receivers and many other unpredictable factors influencing the WLAN signal distributions in indoor environment [25], the characteristics of received SNR should be discussed for the purpose of avoiding multi-mode phenomenon in the process of radio map establishment.

Laptop with Intel PRO/Wireless 3945ABG network connection (Inter-NC1) and D-link DWL-2100AP (AP_i) are selected. WLAN signals are recorded by NetStumbler tool in windows XP system. The sampling frequency is 2 samples per second and 360 samples for each RP with 90 samples per orientation.

(a) Multi-path effect

Two experiments are compared for discussing the multi-path effect. One is in the microwave anechoic chamber and the other experiment is in the real indoor environment.

According to Fig. 7, the SNR distribution is broadened with larger standard deviation in real indoor environment because of the multi-path time delay spread.

(b) Connection states of receivers

Connected and unconnected states between APs and receiver are analyzed in this section. The connected state means that the laptop with Inter-NC1 can go online through the special connected AP. But in one time, the wireless network card can only connect one AP, so for the other detectable but unconnected APs, the network card is

defined in unconnected state. And the SNR distributions for different connection states are shown in Fig. 8.

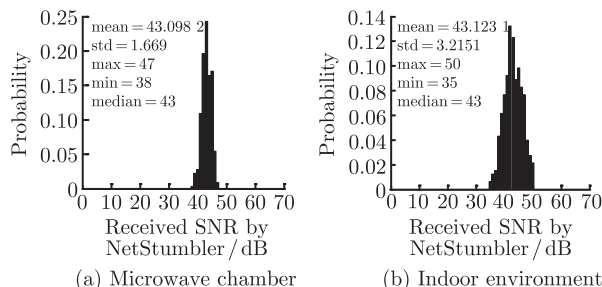


Fig. 7 SNR distribution in different environment

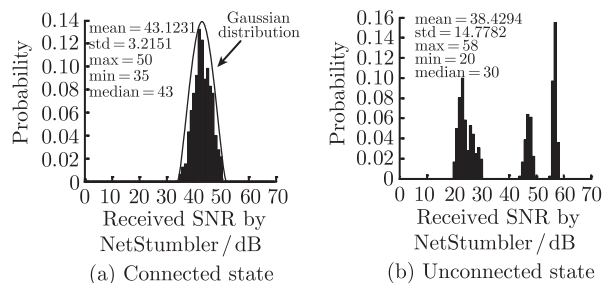


Fig. 8 SNR distribution in different connection states

Based on Fig. 8, multi-mode phenomenon emerges in unconnected state, but for the connected state, the SNR distribution can be approximated by Gaussian or modified left partial Gaussian distribution. Obviously, the connection state is one of the significant reasons of common multi-mode phenomenon.

(c) Interference among adjacent receivers

In this section, another laptop with Intel PRO/Wireless 2200BG Network Connection (Inter-NC2) is used in order to compare the received SNR distribution with the former laptop with Inter-NC1. Two distinguished situations for the different connection states discussed before should be separately analyzed. Interference from Inter-NC2 for Inter-NC1 which is respectively in unconnected and connected state is shown in Fig. 9 and Fig. 10.

According to Fig. 9 and Fig. 10, the interference among adjacent receivers is terrible in unconnected state situation. But for the receiver in connected state, interference from other receivers can be neglected.

(d) Different types of network cards

In order to compare the received SNR distributions by different wireless network cards, Inter-NC1 and Inter-NC2 are respectively utilized to record signal samples from the same AP at the same RP.

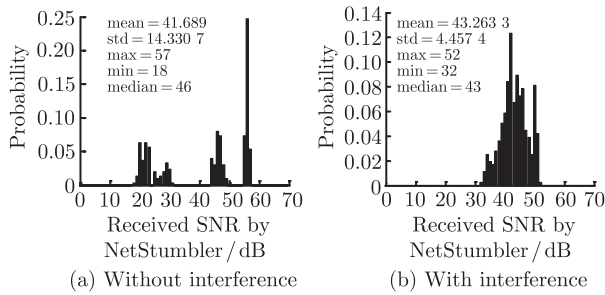


Fig. 9 SNR distribution in unconnected state

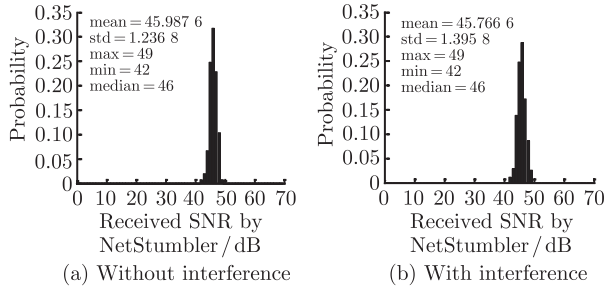


Fig. 10 SNR distribution in connected state

Obviously, different wireless network cards induce different SNR distributions in the real indoor environment. So, in order to decrease the received SNR error generated by different wireless network cards, the laptop with Inter-NC1 is selected as the signal receiver both for the radio map establishment and coordinates' estimation.

According to foregoing discussion about the characteristics of received SNR distribution in WLAN environment, the common multi-mode phenomenon is mainly induced by the following three factors.

- (a) Connection states of receiver.
- (b) Interference between different adjacent receivers in unconnected state.
- (c) Types of wireless network cards.

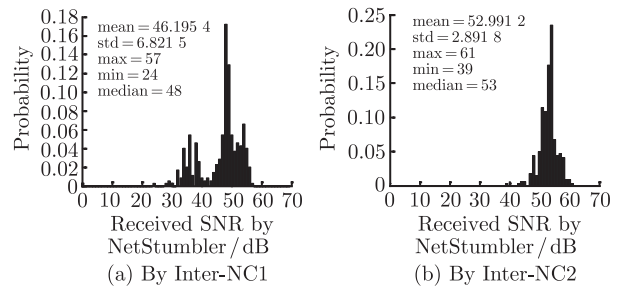


Fig. 11 SNR distribution by different network cards

The former two factors can be avoided by keeping the wireless network cards in the connected state no matter in the off-line phase or in the on-line phase. But the divergence of different network cards will significantly affect the adaptability and extendibility of a radio map based indoor location system.

5. Experiments and analysis

5.1 Experimental setup

Based on the flat of experimental environment shown in Fig. 2, the measurements of RPs are performed for 72 points (locations) which are 1m apart from each other and the test points (56 points in all) are selected in the middle of 4 neighboring RPs.

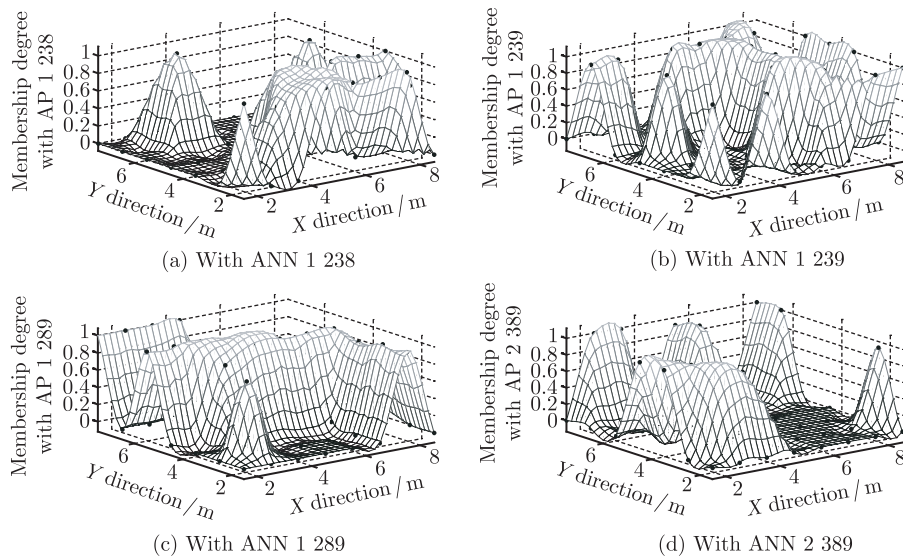


Fig. 12 Membership degrees in X direction

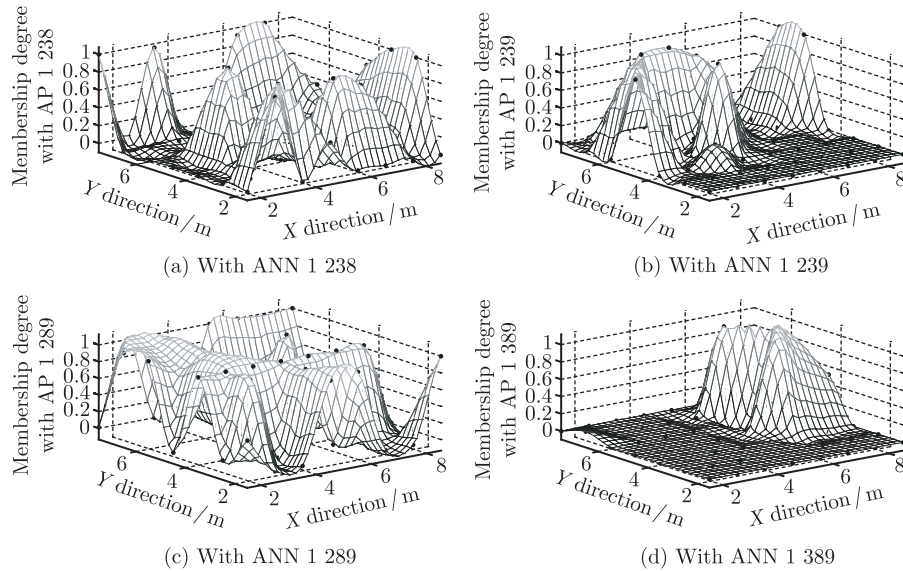


Fig. 13 Membership degrees in Y direction

5.2 Performance results

According to Fig. 6, there is an ANN selector between the first and second layer ANNs. Therefore, the selection criterions in the on-line phase will be discussed firstly.

Criterion 1 Only one output of area division ANN is larger than 0.9.

A unique ANN subsystem corresponding to membership degree larger than 0.9 in layer 2 will be selected to estimate the MT's coordinates.

Criterion 2 More than one output of area division ANN is larger than 0.9.

All the ANN subsystems corresponding to membership

degrees larger than value 0.9 should be considered. And the final estimated coordinates C^* will be the weighted average values calculated by

$$\left\{ \begin{aligned}
 W_i^* &= 0.1 + \frac{(1 - D_i) - \min_j(1 - D_j)}{\max_j(1 - D_j) - \min_j(1 - D_j)} \times (0.9 - 0.1) \\
 C^* = (x^*, y^*) &= \frac{\sum_{i=1}^{N_{ANN}} \frac{1}{W_i^*} \times (x_i, y_i)}{\sum_{i=1}^{N_{ANN}} \frac{1}{W_i^*}}
 \end{aligned} \right. \quad (6)$$

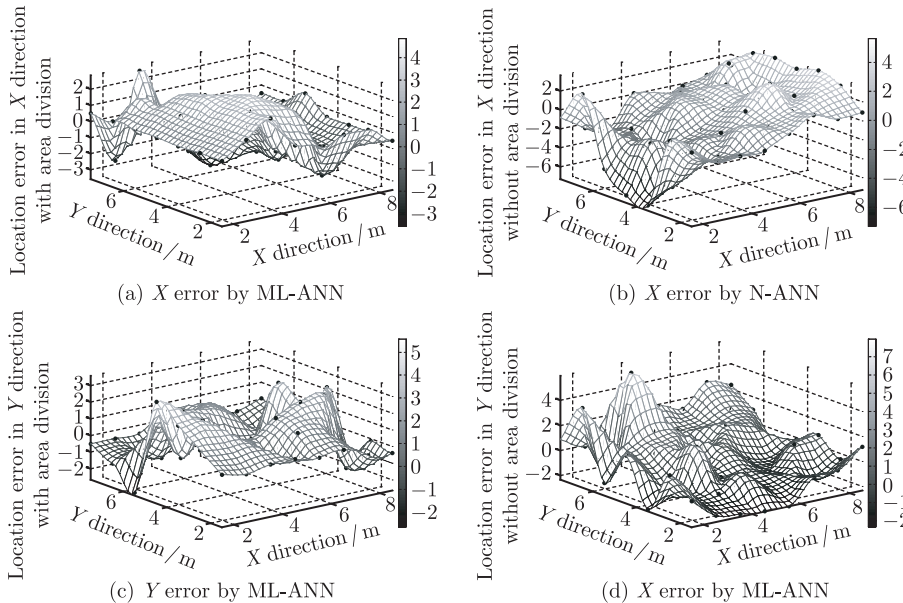


Fig. 14 Location error in different directions

where D_i denotes the membership degree of the i th ANN subsystem. N_{ANN} denotes number of ANN subsystems with membership degrees larger than 0.9.

Criterion 3 All the outputs of area division ANN are smaller than 0.3.

C^* is the weighted average value obtained by all the

ANN subsystems in layer 2.

The accuracy performance of multilayer ANN (ML-ANN) and normal ANN (N-ANN) location methods are shown in Fig. 14 and Fig. 15.

Furthermore, the probabilities of the accumulated error for different types of ANN are also presented by Fig.16.

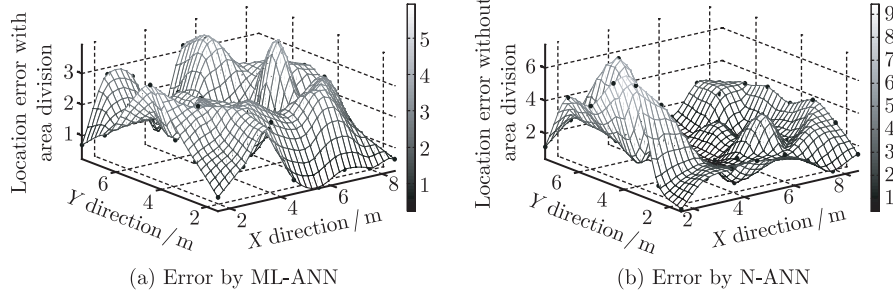


Fig. 15 Total location error by different ANNs

From Fig. 16, the following three conclusions can be obtained.

(a) Multilayer ANN outperforms normal ANN without area division.

(b) The total error is mainly induced by the error in the Y direction for the multilayer ANN location system.

(c) The location error has been limited in 4 m by multilayer ANN, and error in 3 m with confidence probability 92.86% completely satisfies application requirement.

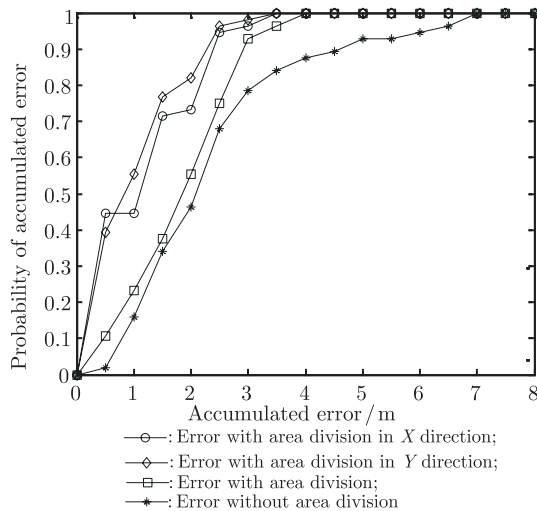


Fig. 16 Probability of accumulated location error

5.3 Experimental comparison

Location performances of KNN and probability methods are also discussed in the same target location area shown in Fig. 2. And mean errors by the KNN method based on different signal characteristics are separately shown in Fig. 17.

Obviously, the KNN method comprises two parameters, the number of neighbors k and distance type q . $q = 1$ denotes the Manhattan distance and $q = 2$ denotes the Euclidean distance. But along with the increase of k and q , the KNN algorithm becomes much more complex. In this paper, the optimal KNN coefficient with $k = 13$ and $q = 1$ is considered.

$$\left\{ \begin{array}{l} D_t = \left(\sum_{i=1}^{N_{AP}} |R_{new,i} - R_{t,i}|^q \right)^{1/q}, \quad t = 1, \dots, 72 \\ \{C^j : C^j \in \text{Seq}_{\min \rightarrow \max}(D_t, k), j = 1, \dots, k\} \\ C^* = (x^*, y^*) = \frac{1}{k} \sum_{j=1}^k (x_j, y_j) = \frac{1}{k} \sum_{j=1}^k C^j \end{array} \right. \quad (7)$$

where $R_{new,i}$ and $R_{t,i}$ denote the new recorded signal and pre-stored fingerprint respectively at RP t . N_{AP} denotes the number of detectable APs in the target location area. $\text{Seq}_{\min \rightarrow \max}(D_t, k)$ denotes the set which consists of the front k elements with the corresponding value D_t in ascending order.

RP C^* satisfying (8) is estimated as the MT's position for the probability method.

$$\left\{ \begin{array}{l} R_{new} = (R_{new,1}, \dots, R_{new,N_{AP}}) \\ P(C^*/R_{new}) = \max_t [P(C^t/R_{new})] = \\ \max_t \left[\frac{P(R_{new}/C^t)P(C^t)}{P(R_{new})} \right] \\ P(R_{new}/C^t) = \prod_{i=1}^{N_{AP}} P(R_{new,i}/C^t), \quad t = 1, \dots, 72 \end{array} \right. \quad (8)$$

where $P(R_{new})$ and $P(C^t)$ are constants.

The location error of the probability method with different accuracy is shown in Fig. 18.

Comparison among multilayer ANN, optimal KNN (Opt-KNN) and probability methods is shown in Table 2. The following two parameters should be defined firstly.

Table 2 Comparison among typical location methods

	ML-ANN	Opt-KNN	Probability
Max-error/m	3.93	5.45	4.50
Min-error/m	0.28	0.05	1.04
Mean-error/m	1.91	1.74	2.93
Median-error/m	1.95	1.90	2.86
E-R/m	1.00	1.00	1.00
$\epsilon_1 = \frac{\text{Mean-error}}{\text{E-R}}$	1.91	1.74	2.93
$\epsilon_2 = \frac{\text{Median-error}}{\text{A-D/m}^2}$	2.02	2.87	1.57
$\epsilon_3 = \text{Median-error} \times (\text{A-D}) / \text{m}$	0.14	0.13	0.12
Storage cost	$3N \sum (\omega, \theta, \rho)$	$N(RPs)$	$2N(RPs)$
Calculation	+ & ×	$\sqrt{\cdot}$ & $ \cdot $	e^x

(a) Error resolution (E-R)

E-R denotes the distance interval between neighboring

RPs. A higher E-R value is much more beneficial to describe the characteristics of signal distribution. However, it also requires a higher time and storage cost for the establishment of radio map.

(b) AP density (A-D)

A-D denotes the number of APs per 1 m² utilized for MT's coordinates' estimation.

Obviously, optimal KNN performs best in the accuracy aspect (except the maximum error). However, the performance of KNN will significantly deteriorate if the coefficients have not been properly selected. Multilayer ANN achieves great location accuracy, but also performs best for the aspects of storage cost and calculation complexity.

Storage cost for the KNN and probabilistic methods depends on the number of RPs. So, if the dimensions of the target area enlarge, the storage cost will significantly increase. But for the multilayer ANN, the number of weights and biases pre-stored is much smaller. And also, the storage cost for the probabilistic method is largest because there are two parameters, mean and variance, which should be pre-stored for each RP.

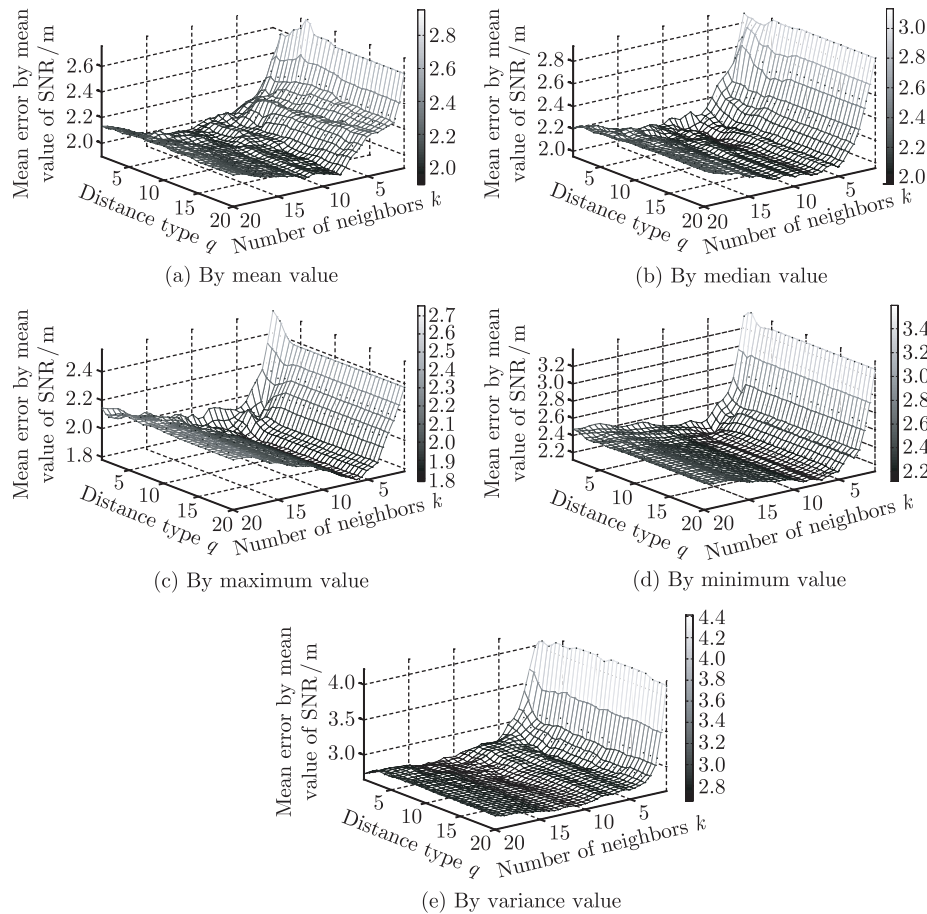


Fig. 17 Location performance by KNN method

Furthermore, only add and multiply operations are needed for multilayer ANN. But for the other two typical indoor location methods, the square root, absolute value

and exponent operations are included. And the traversal for all the RPs is needed which will also increase the time cost.

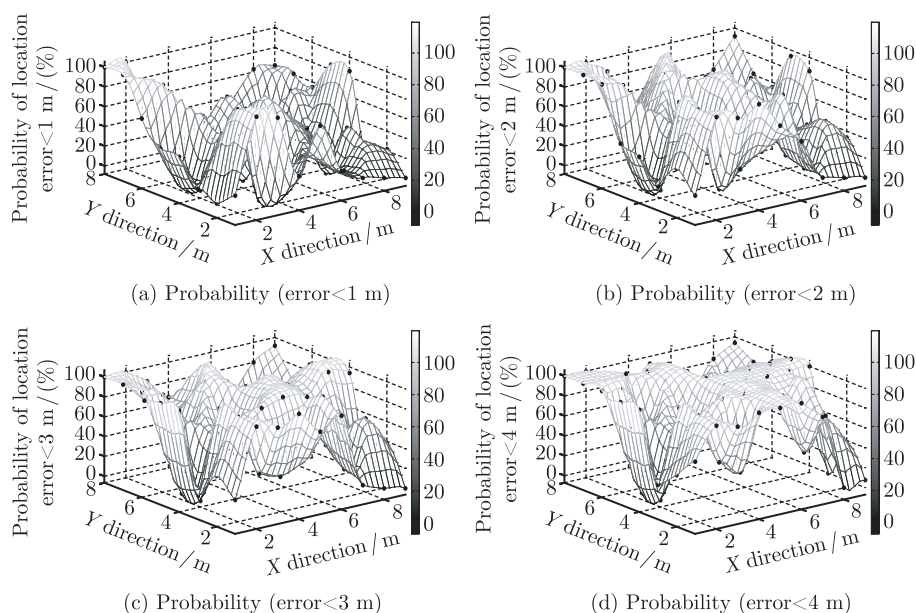


Fig. 18 Location performance by probability method

6. Conclusion

The multilayer ANN indoor location system is investigated in this paper. Firstly, distance relativities for different signal characteristics from separate APs are analyzed in order to optimize the ANN training samples. After this process, the strong signals and noise with poor distance dependence can be eliminated for the purpose of improving the training efficiency and increasing the location accuracy.

Secondly, based on discussion of signal characteristics in different conditions, the avoidance strategy for common multi-mode phenomenon has also been presented.

Finally, compared with the other typical indoor location methods, the achieved mean error 1.91 m and accuracy in 3 m with confidence probability 92.86% can completely satisfy service-based application requirements.

However, reliability of area division ANN in multilayer ANN system and division strategies for irregular location area will be paid much more attention in the future work.

References

- [1] Y. Y. Gu, A. Lo, I. Niemegeers. A survey of indoor positioning systems for wireless personal networks. *IEEE Communications Surveys & Tutorials*, 2009, 11(1): 13–32.
- [2] C. A. Patterson, Muntz R R, C. M. Pancake. Challenges in location-aware computing. *IEEE Pervasive Computing*, 2003, 2(2): 80–89.
- [3] A. M. Ladd, K. E. Bekris, G. Marceau, et al. Using wireless ethernet for localization. *Proc. of IEEE/RSJ International Conference on Intelligent Robots and System*, 2002, 1: 402–408.
- [4] M. Hazas, J. Scott, J. Krumm. Location-aware computing comes of age. *IEEE Computer*, 2004, 37(2): 95–97.
- [5] R. Want, B. Schilit. Expanding the horizons of location-aware computing. *IEEE Computer*, 2001, 34(8): 31–34.
- [6] M. Lashley, D. M. Bevly, J. Y. Hung. Performance analysis of vector tracking algorithms for weak GPS signals in high dynamics. *IEEE Journal of Selected Topics in Signal Processing*, 2009, 3(4): 661–673.
- [7] L. M. B. Winternitz, W. A. Bamford, G. W. Heckler. A GPS receiver for high-altitude satellite navigation. *IEEE Journal of Selected Topics in Signal Processing*, 2009, 3(4): 541–556.
- [8] A. H. Sayed, A. Tarighat, N. Khajehnouri. Network-based wireless location: challenges faced in developing techniques for accurate wireless location. *IEEE Signal Processing Magazine*, 2005, 22(4): 24–40.
- [9] U. Ahmad, A. Gavrilov, L. Sungyoung, et al. Modular multi-layer perceptron for WLAN based localization. *Proc. of International Joint Conference on Neural Networks*, 2006: 3465–3471.
- [10] Q. X. Pang, S. C. Liew, V. C. Leung, et al. Design of an effective loss-distinguishable MAC protocol for 802.11 WLAN. *IEEE Communications Letters*, 2005, 9(9): 781–783.
- [11] S. Nattapong, P. Krishnamurthy. Location fingerprint analyses toward efficient indoor positioning. *Proc. of 6th Annual IEEE Conference on Pervasive Computing and Communications*, 2008: 100–109.
- [12] K. Kaemarungsi. Efficient design of indoor positioning systems based on location fingerprinting. *Proc. of International Conference on Wireless Networks, Communications and Mobile Computing*, 2005, 1: 181–186.
- [13] K. Derr, M. Manic. Wireless based object tracking based on neural networks. *Proc. of IEEE Conference on Industrial Electronics and Applications*, 2008: 308–313.
- [14] M. Borenovic, A. Neskovic, D. Budimir, et al. Utilizing artificial neural networks for WLAN positioning. *Proc. of IEEE*

19th International Symposium on Personal, Indoor and Mobile Radio Communications, 2008: 1–5.

- [15] S. H. Fang, T. N. Lin. Indoor location system based on discriminant-adaptive neural network in IEEE 802.11 environments. *IEEE Trans. on Neural Networks*, 2008, 19(11): 1973–1978.
- [16] Y. B. Xu, M. Zhou, L. Ma. WIFI indoor location determination via ANFIS with PCA methods. *Proc. of IEEE International Conference on Network Infrastructure and Digital Content*, 2009: 647–651.
- [17] U. Ahmad, A. Gavrilov, S. Lee, et al. Modular multilayer perceptron for WLAN based localization. *Proc. of International Joint Conference on Neural Networks*, 2006: 3465–3471.
- [18] K. Hornik. Approximation capabilities of multilayer feedforward neural networks. *Archive*, 1991, 4(2): 251–257.
- [19] D. X. Zhang, Y. Liu, Z. Q. Wang. Generalization enhancement of feedforward neural networks based on the convergence of shape errors. *Proc. of International Conference on Machine Learning and Cybernetics*, 2005, 7: 4054–4059.
- [20] A. Yamazaki, T. B. Ludermit, M. C. P. de-Souto. Global optimization methods for designing and training neural networks. *Proc. of VII Brazilian Symposium on Neural Networks*, 2002: 136–141.
- [21] J. Zhang. A training method for enhancing neural network model generalization. *Proc. of Joint Conference on Neural Networks*, 2002, 1: 800–805.
- [22] C. Y. Tsai, S. Y. Chou, S. W. Lin, et al. Location determination of mobile device for indoor WLAN application using neural network. *Proc. of 4th Conference on Intelligent Environments*, 2008: 1–8.
- [23] M. Stella, M. Russo, D. Begusic. Location determination in indoor environment based on RSS fingerprinting and artificial neural network. *Proc. of International Conference on Telecommunications*, 2007: 301–306.
- [24] I. Vilovk, B. Z. Cihlar. WLAN location determination model based on the artificial neural networks. *Proc. of 47th International Symposium on ELMAR*, 2005: 287–290.
- [25] M. A. Alvarez-Cabanillas. Indoor propagation of diffracted sig-

nals. *Proc. of IEEE Society Symposium on Antennas and Propagation*, 2006: 2181–2184.

Biographies



Mu Zhou was born in 1984. He received the B.S. degree in applied mathematics in 2006, and the M.S. degree in Information and Communication Engineering in 2008, both from Harbin Institute of Technology (HIT). Now, he is pursuing the Ph.D. degree in information and communication engineering. His current research interests include the WLAN indoor artificial location system and wireless communications.
E-mail: zm_llj@163.com



Yubin Xu was born in 1954. He received the B.S. degree in radio measurement in 1986, the M.S. degree in electronics and communication system in 1993, and Ph.D. degree in electronics and communication system, in 2005, all from HIT. He is currently a professor. His research interests include wireless positioning, radio-wave propagation, and mobile communications.
E-mail: ybxu@hit.edu.cn



Li Tang was born in 1985. She received the B.S. and M.S. degrees in information and communication engineering, separately in 2007 and 2009, both from HIT. She is currently working in Alcatel-Lucent Shanghai Bell Ltd. Her interests include optical and mobile broadband networks.
E-mail: tangli123@gmail.com